2 Photonuclear reactions

The beginning of photonuclear research dates back to 1934. In this year Chadwick and Goldhaber[95] published a report about photon reaction of deuterium bombarded with gamma rays of ^{208}Tl (E = 2.62 MeV)[96]. In the same year two papers about photoneutron reaction of ^{7}Be were published by Gentner[97] and Szilard and Chalmers[98], respectively. Until the general availability of betatrons with high electron energy output in the beginning of the 1940´s[99,100], the only photonuclear reactions which could be studied were the photodisintegration processes in deuterium and beryllium since only these elements (except several easily fissile nuclei undergoing photofission reactions at low incident energies) have low enough threshold energies to be disintegrated by photons from gamma-emitting radionuclide sources. One exception is the work of Bothe and Gentner[101] who used promptly emitted gamma-rays from proton reactions as an activating source (see 2.2 and 3.1).

The first report about the detection of an individual nuclear energy level was published - as far as the authors know - in 1939[102]. The first message about isomeric photoexcitation dates back to 1941[103].

Systematic work about photonuclear reactions started in the 1950´s[104] using betatrons, and exact data were established in the beginning of the 1960´s[105, 106], utilising quasi-monoenergetic photons produced through annihilation-in-flight of linac-produced positrons.

Apparently the first analytical application of photon reactions dates back to 1936[3] as was mentioned in Ch.1.

2.1 General features of photonuclear reactions

2.1.1 The absorption of photons by nuclei

Nuclear reactions induced by electromagnetic radiation can be described - at least for sufficiently low photon energies - in terms of a two-stage process. Absorption of a photon leads to an intermediate highly excited state of the nucleus. The excitation energy of this so-called compound nucleus can then be released by emission of photons, neutrons or charged particles. The total cross section for absorption of photons by nuclei shows some very pronounced figures (Fig. 2.1).

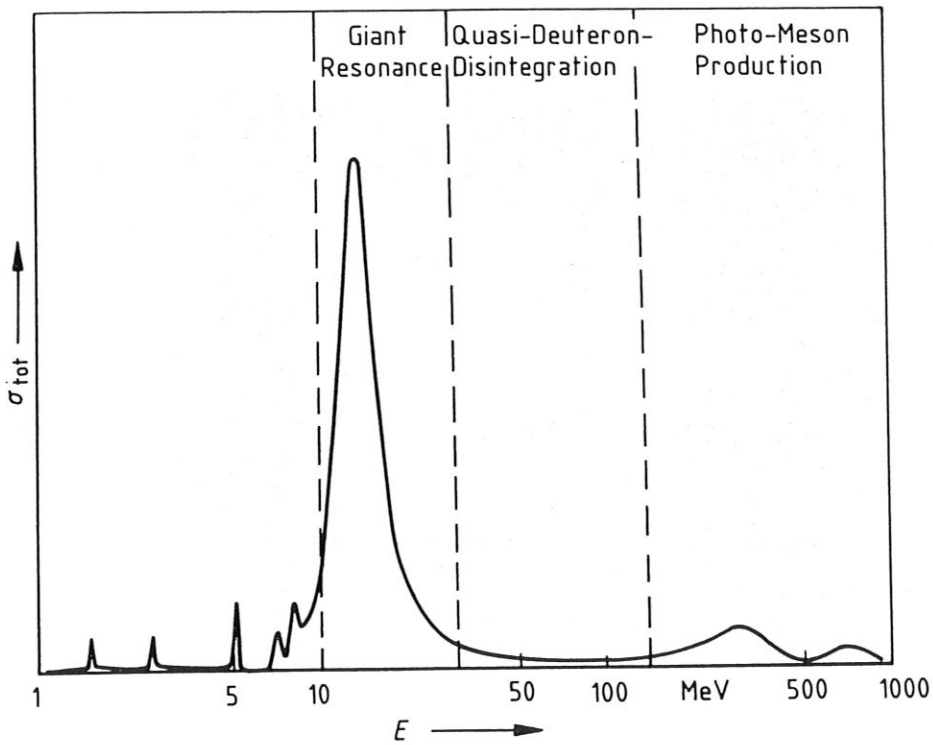

Fig. 2.1: Schematic representation of the total cross section for the absorption of photons by nuclei

2.1.1.1 Excitation of individual nuclear levels

At energies below about 10 MeV isolated nuclear energy states are excited. If the incident photon has just the "right" energy to excite a single nuclear level the total absorption cross section sharply rises to a narrow resonance peak.

From the theory of interaction between electromagnetic radiation and nuclei one obtains the following expression for the absorption cross section of one individual nuclear level:

$$\sigma_a = \sigma_m \cdot \frac{\frac{1}{4} \cdot \Gamma_a^2}{(E - E_a)^2 + \frac{1}{4} \cdot \Gamma_a^2} \qquad (2.1)$$

σ_m = peak cross section. It depends on the photon wavelength at resonance and the properties of the excited and the ground state of the nucleus.

E = energy of the incident photons

E_a = resonance energy (energy of the excited state)

Γa = total energy width of the excited state a. The energy width of the nuclear level is proportional to the transition probability from this level to all other lower states.

$$\sigma_m = \frac{\lambda^2}{2\pi} \cdot \frac{2I_a + 1}{2I_g + 1} \cdot \frac{\gamma_g}{\Gamma_a} \qquad (2.2)$$

λ = photon wavelenght at resonance

I_a, I_g = spins of the excited and the ground state respectively

γ_g = partical width of the excited state a for the transition to the ground state g. γ_g is proportional to the transition probability from the excited state a to the ground state g.

The second term in eq. (2.2) represents a resonance curve with Γa being its full width at half maximum. In general, according to the low energy width of nuclear levels (1 eV) the resonance is very sharp. Therefore, although the peak cross section may exceed 10^3 barn, the integrated absorption cross section

for a single level is low. By integrating the resonance term in eq. (2.1) we obtain:

$$\int_0^\infty \sigma \, dE = \sigma_m \cdot \frac{\pi}{2} \cdot \Gamma_a = \frac{\lambda^2}{4} \cdot \frac{2I_a + 1}{2I_g + 1} \cdot \gamma_g \qquad (2.3)$$

Inserting typical values for the photon wavelength at MeV energies and for the ground state radiation width γ_g eq. (2.3) yields values of the order of magnitude of μb · MeV[107].

2.1.1.2 Giant dipole resonance

In the energy range from 10 MeV up to about 30 MeV a very broad resonance maximum is observed in the total photon absorption cross section. In contrast to the excitation of isolated nuclear energy levels at lower photon energies the so-called giant resonance is characterised by a collective vibrational motion of all protons and neutrons within the nucleus. The most important contribution to the giant resonance excited by photons is due to the electric dipole mode. The electric giant dipole resonance is generally interpreted as a collective motion of all protons against all neutrons. The schematic representation given in Fig. 2.2a for a spherical nucleus shows that in this vibrational mode all protons together move with respect to the total of the neutrons under the influence of the periodic electric field. Since the nucleus is assumed to be spherically symmetric no direction of vibrational motion is favoured and therefore the resonance frequencies for the three degrees of freedom are identical. For spherical nuclei therefore only one single broad resonance maximum is observed in the total photon absorption cross section.

If the nucleus in its ground state has a permanent deformation the structure of the giant resonance becomes more complicated because the resonance frequencies for the three degrees of freedom are different. In Fig. 2.2b a prolate nucleus (cigar shape) is shown. Obviously there are two vibrational directions with different resonance frequencies namely the motions in z-direction and perpendicular to the z-direction. The vibrational modes in x-and y-direction are degenerate. Therefore the giant dipole resonance curve is composed of two resonance curves centered at different photon energies. In the case of prolate nuclei the higher frequency component has the twofold intensity whereas for oblate nuclei (earth shape) the lower component is more intense. Thus the total photon absorption cross section of deformed nuclei exhibits a resonance maximum

with two distinct peaks.

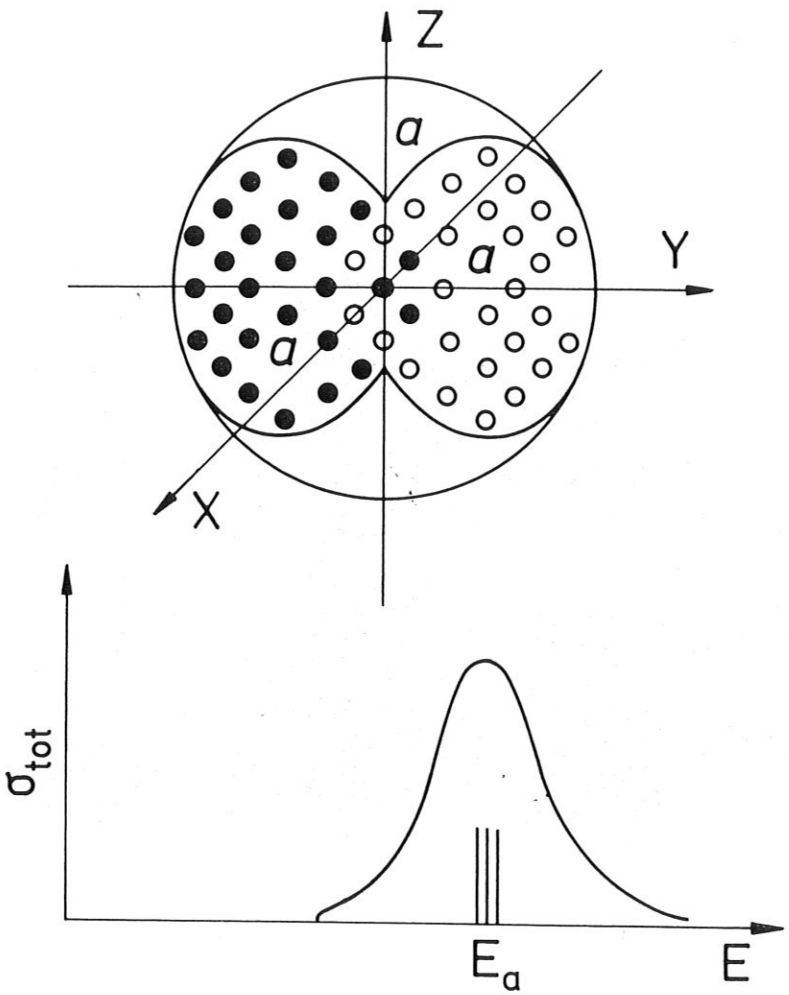

Fig. 2.2a: Schematic representation of the collective motion of all protons against all neutrons in the electric giant dipole resonance vibration mode (upper figure) for spherical nuclei and the typical shape of the electric giant dipole resonance absorption cross section (lower figure)

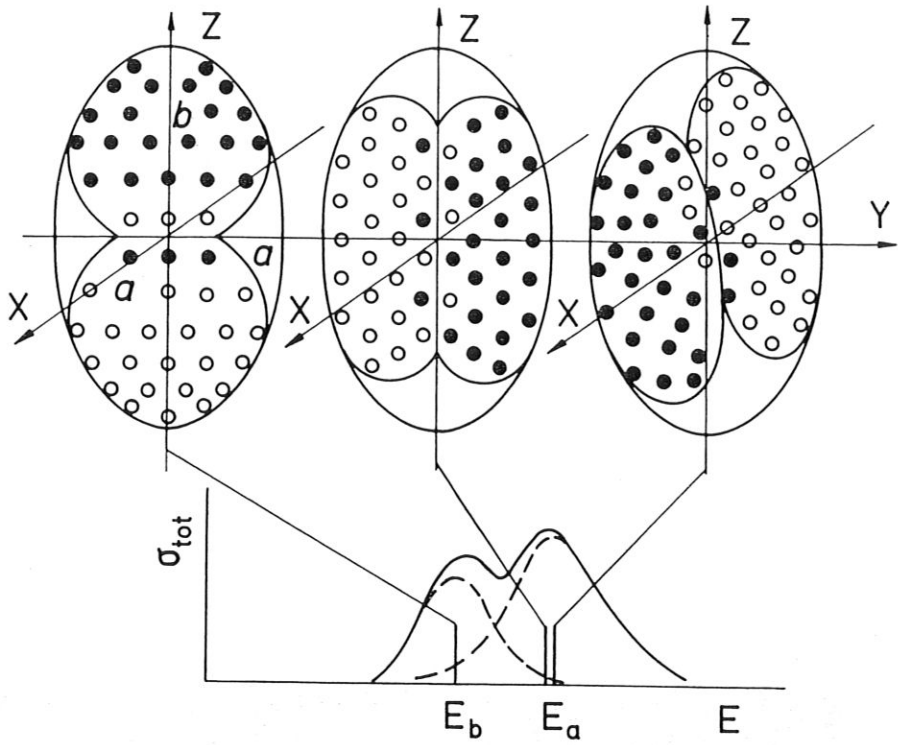

Fig. 2.2b: Schematic representation of the different electric giant dipole resonance vibration modes (upper figure) and the absorption cross section function (lower figure) for deformed nuclei (prolate = cigar-shaped)

The semiclassical theory of the interaction of photons with nuclei yields the following expression for the giant resonance curve:

$$\sigma_a(E) = \sigma_m \cdot \frac{E^2 \cdot \Gamma^2}{(E_m^2 - E^2)^2 + E^2 \cdot \Gamma^2} \qquad (2.4)$$

σ_m = peak cross section
E = energy of the incident photons
E_m = resonance energy
Γ = width of the giant resonance (full width at half maximum)

Expression (2.4) is a Lorentz curve (for the meaning of the parameters see also Fig. 2.2).

In the case of deformed nuclei the doubly peaked resonance curve is readily described by the superposition of two Lorentz curves:

$$\sigma_a(E) = \sigma_{m_1} \cdot \frac{E^2 \cdot \Gamma_1^2}{(E_{m_1}^2 - E^2)^2 + E^2 \cdot \Gamma_1^2} + \sigma_{m_2} \cdot \frac{E^2 \cdot \Gamma_2^2}{(E_{m_2}^2 - E^2)^2 + E^2 \cdot \Gamma_2^2} \qquad (2.5)$$

(see Fig. 2.2b).

The theory of the interaction of electromagnetic radiation with nuclei yields an interesting expression for the integrated cross section of the electric giant dipole absorption:

$$\int_0^\infty \sigma_a(E)\,dE = 60 \cdot \left(\frac{N \cdot Z}{A}\right) \quad [\text{MeV} \cdot \text{mbarn}] \qquad (2.6)$$

N = number of neutrons in the nucleus
Z = number of protons
A = Z + N = mass number

The comparison of this relationship with experimentally obtained total integrated photon absorption cross sections shows that the electric giant dipole resonance is the most important contribution to the total photon absorption cross section. The contribution of other vibrational modes is generally small. From eq. (2.6) we easily derive that the integrated cross section increases with increasing atomic number Z of the target nuclei.

The resonance energy E_m slowly decreases with increasing mass number:

$$E_m \approx (40 \cdot A^{-\frac{1}{3}} + 7.5)\ \text{MeV} \qquad (2.7)$$

E_m ranges from about 24 MeV in ^{16}O to 13,5 MeV for ^{208}Pb. The width Γ varies between 4 MeV and 8 MeV for medium and heavy nuclei. The peak cross section strongly increases with increasing mass number from less than 10 mbarn up to

about 500 mbarn.

Further recommended literature about the Giant Dipole Resonance can be found in Ref's.[108-115].

2.1.1.3 Interaction with high energy photons

Beyond the giant resonance region (E > 30 MeV) other interaction mechanism become important. If a high energy photon is absorbed instead of a collective excitation of all nucleons the interaction with individual nucleons is observed. The magnitude and the energy dependency of the total absorption cross section can be interpreted in terms of the so-called quasi-deuteron disintegration. Within the framework of this model one assumes that the photon interacts with a correlated neutron-proton pair (deuteron) inside the nucleus giving rise to direct nucleon emission without participation of the other nucleons. Due to the interaction of the high energy photon with only a small number of nucleons the absorption cross section is quite low as compared with the giant resonance region (Fig. 2.1).

Finally, photons with energies above 140 MeV can produce π-mesons. Due to photomeson productions the total absorption cross section rises again beyond the threshold of this process (Fig. 2.1).

2.1.2 The deexcitation of the nucleus after absorption of a photon

The excitation energy may be released from the nucleus by

- reemission of a photon with the same energy as the incident photon. This process is called elastic scattering or (γ,γ)-reaction.

- emission of photons with lower energy. This reaction type is known as inelastic photon scattering or (γ,γ')-reaction[179].

- emission of neutrons, protons or composite charged particles if the excitation energy of the nucleus exceeds the particle separation threshold.

In photon activation analysis, besides the photodisintegration process, only reactions with particle emission and to a minor extent inelastic photon scattering have been used because these reaction types may produce permanent radioactivity in the sample to be analysed which can be conveniently measured.

2.2 (γ,γ')-reactions

The physical mechanism of inelastic photon scattering can be readily understood using a simplified energy level diagram of the nucleus (Fig 2.3). The nucleus is excited by absorption of a photon with the appropriate energy corresponding to the energy difference between the isolated level and the ground state g (resonance absorption). In general the excited nuclear states have a very short lifetimes (typically $\lesssim$ 1 ns) decaying into lower levels or directly into the ground state.

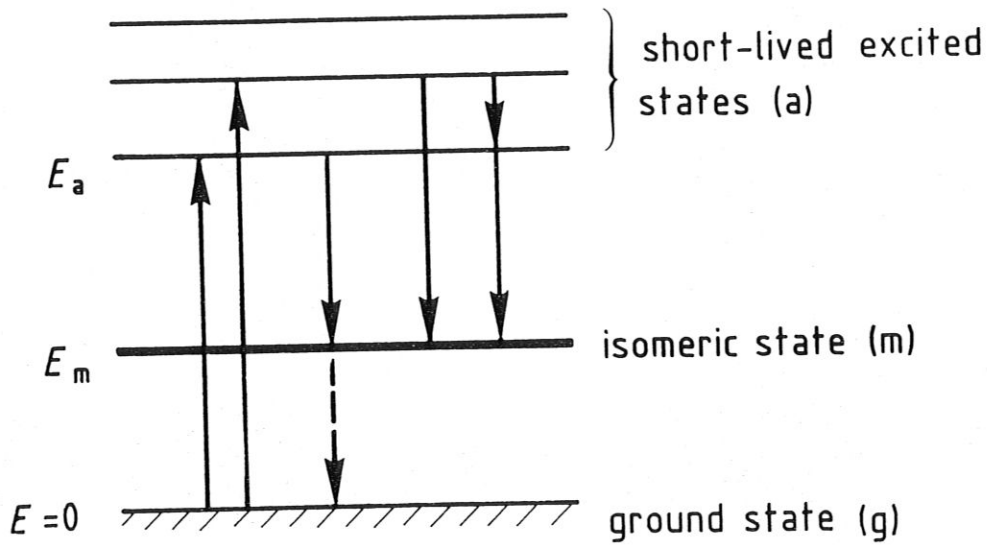

Fig. 2.3: Simplified energy level diagram of a nucleus having an isomeric state

In a considerable number of nuclides, however, an isomeric state exists which is characterised by its abnormally long lifetime. Due to the very low transition probability the half-life of an isomeric state may be as high as several tens of years. If such a nucleus is excited by resonant photon absorption the decay of the short-lived state a may lead to the isomeric state m. The decay of the isomeric state can then be measured after irradiation due to its sufficiently high lifetime using conventional photon spectroscopy.

This interaction mechanism is called inelastic scattering because the reemitted photons have lower energy than the exciting primary ones. The cross section for the inelasting scattering via an isomeric state is obtained from the absorption cross section by multiplying with the relative transition probability from the absorbing state a to the isomeric state m:

$$\sigma_{in} = \sigma_a \cdot \frac{\gamma_m}{\Gamma_a} \tag{2.8}$$

σ_m = partial widths of the excited state a for the transition to the isomeric state m

Γ_a = total width of the excited state a for transitions to all other (lower) states

From eq. (2.1) and eq. (2.2) we obtain:

$$\sigma_{in} = \frac{\lambda^2}{2\pi} \cdot \frac{2I_a + 1}{2I_g + 1} \cdot \frac{\gamma_g \cdot \gamma_m}{\Gamma_a^2} \cdot \frac{\frac{1}{4} \cdot \Gamma_a^2}{(E - E_a)^2 + \frac{1}{4} \cdot \Gamma_a^2} \tag{2.9}$$

The integrated (γ,γ') cross section follows from eq. (2.3):

$$\int_0^\infty \sigma_{in}\, dE = \frac{\lambda^2}{4} \cdot \frac{2I_a + 1}{2I_g + 1} \cdot \frac{\gamma_g \cdot \gamma_m}{\Gamma_a} \tag{2.10}$$

From eq. (2.10) one obtains for typical nuclear data an integrated (γ,γ') cross section for a single level a below 10^{-6} · barn · MeV, in agreement with experiment. This value is much lower than the corresponding intgrated cross sections of e.g. photoneutron reactions. Therefore, the achievable specific activity induced in the sample by (γ,γ')-reactions is much lower than for e.g. (γ,n)-reactions and, consequently, the analytical sensitivity using (γ,γ')-reactions is poor.

Another difficulty arises from the fact that inelastic photon scattering requires resonance absorption of the incident photon by the nucleus. Excitation of an isolated nuclear energy level is only possible if the difference between the incident photon energy and the energy of the excited state is much less

than 1 eV. This problem can be overcome using a continuous primary photon spectrum containing photons over a wide energy range. A suitable continuous source is "bremsstrahlung" radiation (X-rays) which is produced when high energy electrons are absorbed in a heavy metal target. Therefore, electron accelerators can be conveniently used for activation analysis using (γ,γ')-reactions. The maximum energy of the bremsstrahlung photons varies linearly with the electron energy. With increasing electron energy successively higher nuclear energy levels a can be excited. If there are two states which can be excited from the ground state and decay (directly or via a cascade) into the isomeric level (Fig. 2.3) the activation curve (specific activity of the isomer as a funktion of electron energy) will consist of two parts with distinctly different slopes.

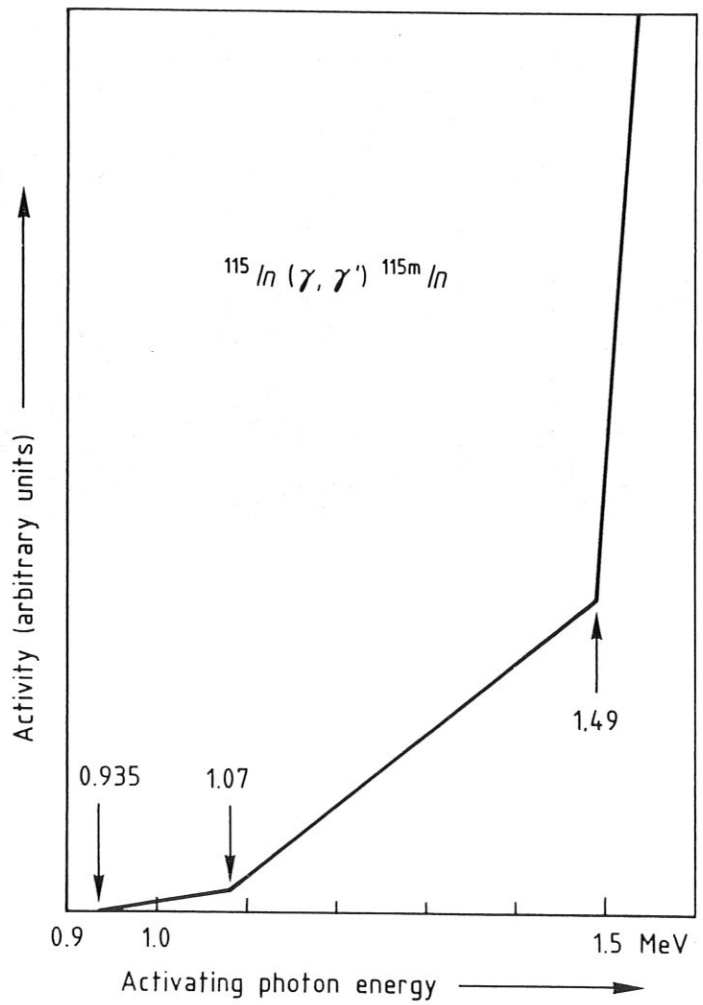

Fig. 2.4: Typical yield curve for a (γ,γ')-reaction excited by bremsstrahlung as a function of the maximum photon energy (taken out of Ref.[122])

The first reaction is due to excitation of the lower level. If the electron energy reaches the energy of the next level additional transitions to the isomeric state are induced, therefore the slope of the activation curve rises at this energy. Fig. 2.4 shows a typical measurement of the activation curve for the re-action $^{115}In(\gamma,\gamma')^{115m}In$ which clearly exhibits various bending points corresponding to the different excited levels of ^{115}In decaying into the 336 keV isomeric state. The general increase of the specific activity of the isomer is due to the higher yield of bremsstrahlung photons at increasing electron energy.[116]

High activity ^{60}Co gamma-ray sources have also been used for inelastic scattering (see also Ch.3). In this case primary ^{60}Co γ-rays (1,17 MeV and 1,33 MeV) do not directly contribute to the excitation of the nuclei. However, a continuous spectrum of photons with lower energy is produced by Compton scattering of the primary photons in the source material itself and in additional scatterers placed in front of the source.

The third method is based on the by-chance coincidence of γ-ray energies. By capture of thermal neutrons from a reactor a large number of γ-rays over a wide energy range (up to about 8 MeV) can be obtained from a large variety of target elements exposed to the neutron beam. Some of these lines may have just the "right" energy to be resonantly absorbed in the nuclide to be analysed (see 3.1 below).

For more information about isomeric state photoexcitation the reader might refer to Ref's.[116-124,180].

2.3 Photoneutron reactions

If the excitation energy of the nucleus is higher than the binding energy of a nucleon (neutron, proton) or a heavier particle e.g. an α-particle, a neutron or a charged particle may be emitted from the nucleus instead of electromagnetic radiation. Fig. 2.5 shows schematically the total absorption cross section in the photon energy region up to 25 MeV for a nucleus with medium atomic number.

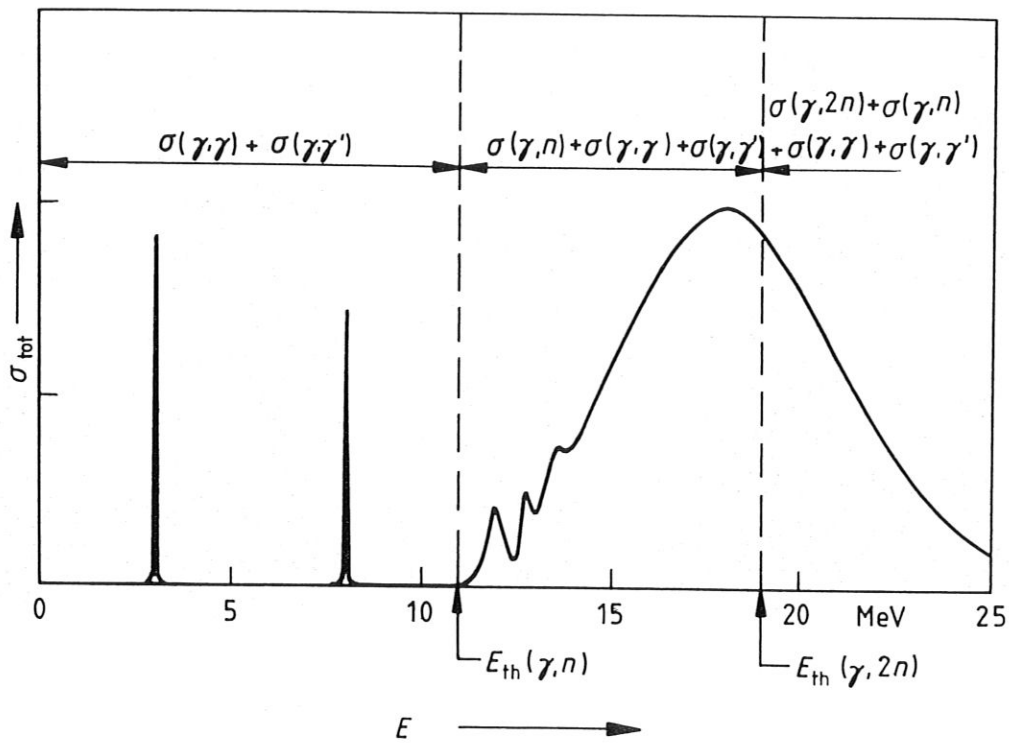

Fig. 2.5: Schematic representation of the low energy part of the total photon absorption cross section function for a nuclide of medium atomic number

Below the nucleon emission threshold - E_{th} (γ,n) - only elastic and inelastic scattering contribute to the total photon absorption cross section which exhibits a few isolated absorption lines in this region. At higher energy the excited nuclear state may decay by photon or nuclear emission. Due to the very

short lifetime of levels above the nucleon emission threshold the absorption lines become increasingly broad. At even higher energy the nuclear level spacing is so small that the excited states partially overlap and the photon absorption leads to collective excitation of all nucleons. This is the giant resonance region already discussed above.

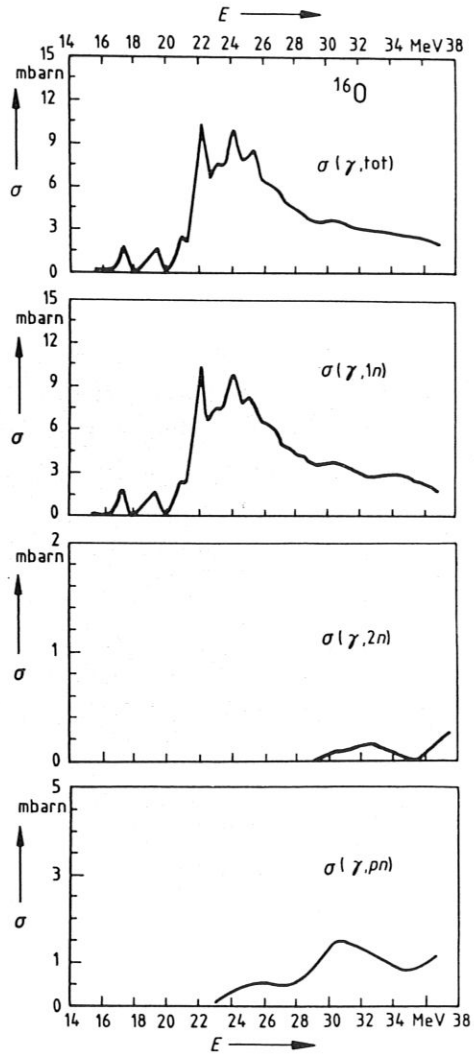

Fig. 2.6: Photoneutron cross sections for ^{16}O; $\sigma(\gamma,\text{tot}) = \sigma(\gamma,\text{tot n})$ = total photoneutron cross section (see Eq. 2.11; after Berman[174])

The total cross section in the giant resonance region is composed of the contributions of elastic and inelastic scattering and emission of a single nucleon, more than one nucleon or a composite charged particle. For medium and

heavy nuclei where the emission of protons and other charged particles is inhibited by the coulomb barrier (see 2.3.3). Here the total photon absorption cross section is nearly completely given by the total photoneutron cross section. For analytical purpose the simplest photoneutrons reaction type (γ,n) is most important.

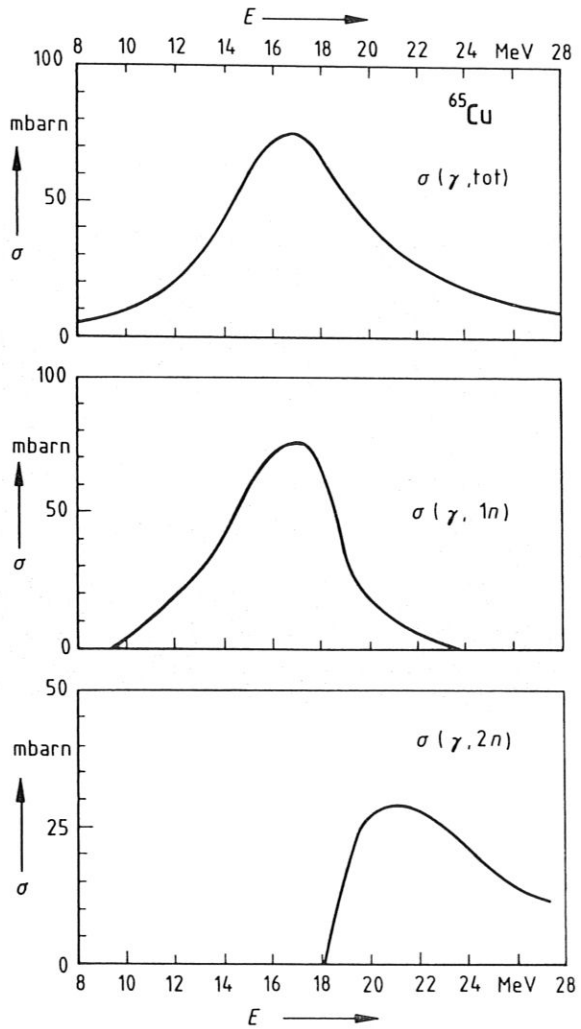

Fig. 2.7: Photoneutron cross sections for ^{65}Cu; explanations see Fig. 2.6

In Fig's. 2.6 to 2.9 typical measured cross section are shown. The upper curve respectively represents the total neutron production cross section and the other ones the partial cross sections for the emission of one neutron, more

than one neutron and charged particles.

$$\sigma(\gamma, \text{tot n}) = \sigma(\gamma, \text{n}) + \sigma(\gamma, \text{np}) + \sigma(\gamma, 2\text{n}) + \sigma(\gamma, 2\text{np}) + \sigma(\gamma, 3\text{n}) + \ldots \quad (2.11)$$

From Fig. 2.6 we see that the reaction $^{16}O(\gamma,n)^{15}O$ is the dominant contribution to the total photoneutron cross section of ^{16}O. Higher order reactions are of minor importance.

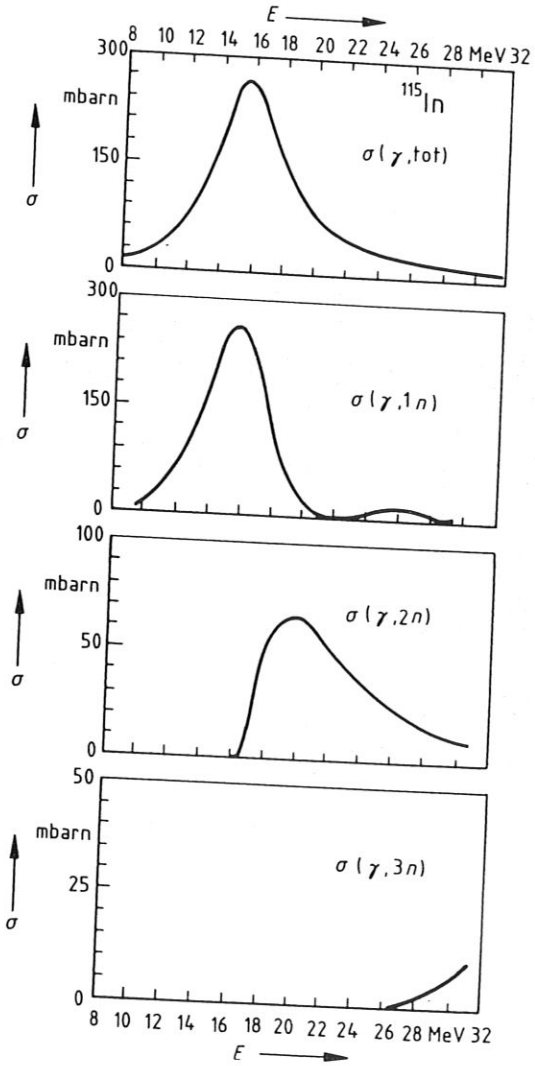

Fig. 2.8: Photoneutron cross sec ions for ^{115}In; explanations see Fig. 2.6

One clearly notes the giant resonance structure in the (γ,n) cross section as well as the contribution of several isolated nuclear levels. The total photoneutron cross section curve for the medium nucleus ^{65}Cu has the very regular and smooth shape of a broad resonance curve (Fig. 2.7) The partial (γ,n)-cross section curve has an asymmetric shape. Above 18 MeV the reaction $^{65}Cu(\gamma,2n)^{63}Cu$ significantly contributes to the total photoneutron cross section of ^{65}Cu. This is also true for the heavier nuclide ^{115}In (Fig. 2.8).

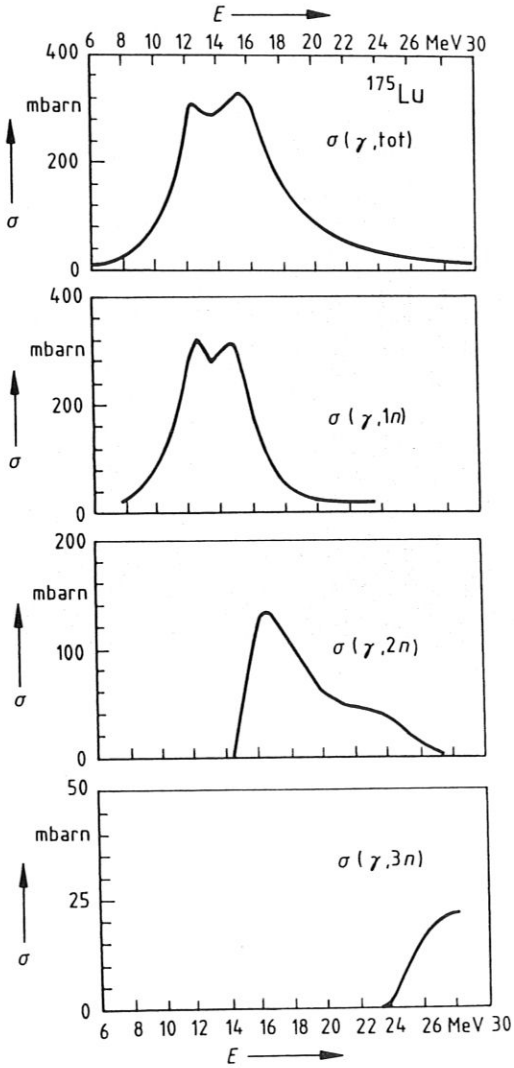

Fig. 2.9: Photoneutron cross sections for ^{175}Lu; explanations see Fig. 2.6

In the case of ^{175}Lu (Fig. 2.9) which is a permanently deformed nucleus we clearly note the influence of the nonspherical shape on the giant resonance curve. Since the ^{175}Lu nucleus is prolate the giant resonance is composed of a low energy component and a high energy component with higher intensity (see Fig. 2.2 b).

If fissile nuclei are highly excited by photon absorption deexcitation by fission is an important reaction mechanism. As an example Fig. 2.10 shows the photofission cross section of ^{238}U in addition to the partial cross section (γ,n) and $(\gamma,2n)$. Photofission contributes significantly to the total reaction cross section[125-127].

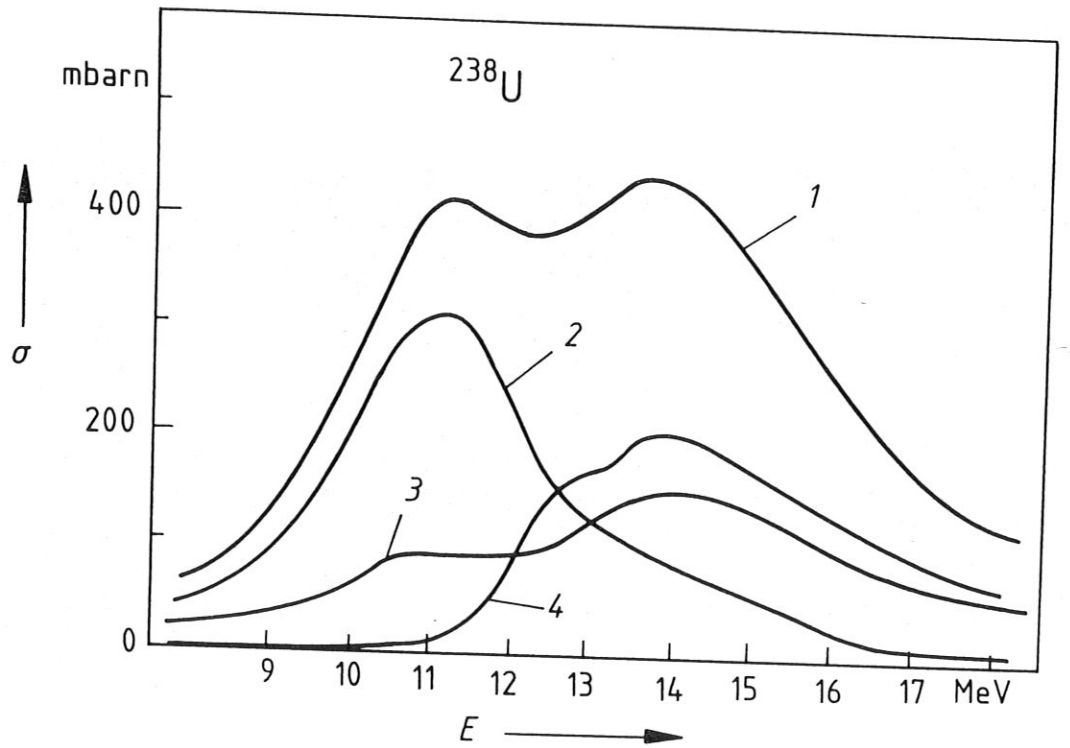

Fig. 2.10: Photonuclear reaction cross sections for ^{238}U; 1 - total photoneutron cross section, 2 - (γ,n)-cross section, 3 - (γ,f)-cross section, 4 - $(\gamma,2n)$-cross section (after Bergère et al.[127])

In Fig. 2.11 to Fig. 2.13 some parameters are plotted which describe the properties of the giant resonance structures observed in the $(\gamma,$ tot n) cross

sections. Fig. 2.11 shows the variation of the center energy E_m of the resonance curve as a function of the atomic number.

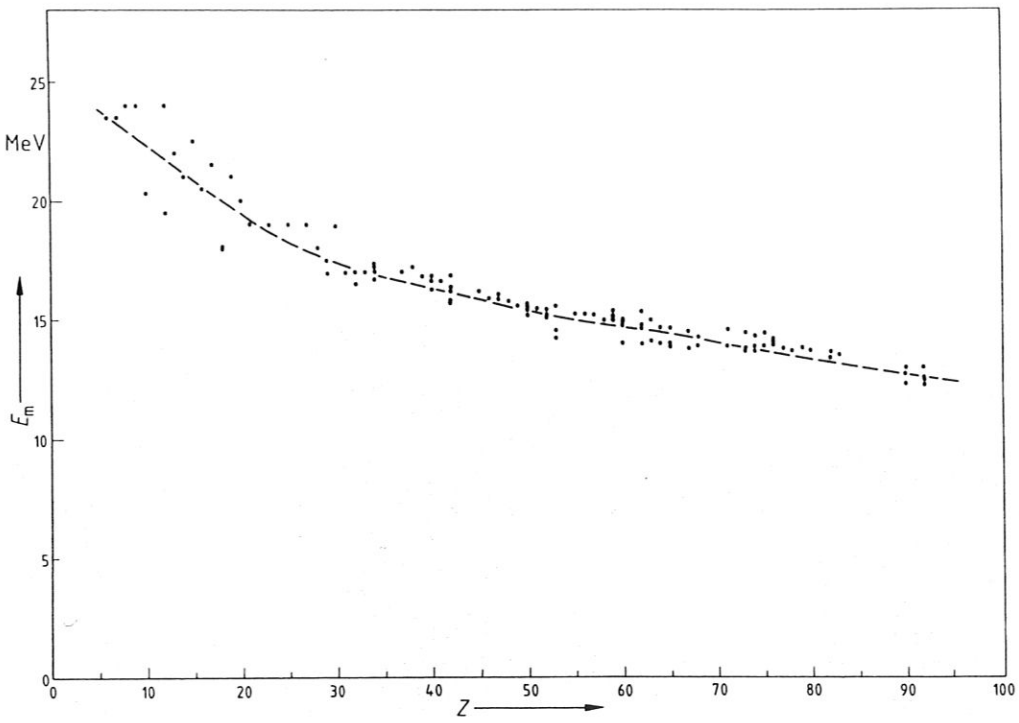

Fig. 2.11: Center energy of the giant dipole resonance cross section as a function of the atomic number

The resonance energy decreases monotonically from about 24 MeV for the light elements to about 12 MeV for the heaviest nuclei. The peak cross section σ_{max} (maximum of the cross section curve), however, strongly increases with the atomic number from less than 10 mbarn up to about 600 mbarn (Fig. 2.12). In contrast to these two parameters the width Γ of the resonance (full width at half maximum) does not exhibit a regular behaviour but strong oscillations as a function of the atomic number (Fig. 2.13). This nonmonotonic structure is correlated with the deformation of the nuclei. If the shape of the nucleus is not spherical - cigar shape (prolate) or earth shape (oblate) - the giant resonance curve is a superposition of two resonance curves with different center energies as was discussed above. The resultant cross section curve then has an irregularly large total width. The dependency of the deformation and thus the giant resonance width on the nucleon number clearly reflects the shell struct-

ure of the nuclei. If proton and neutron shells are closed the nucleus is spherical, otherwise the nucleus may have a permanent deformation.

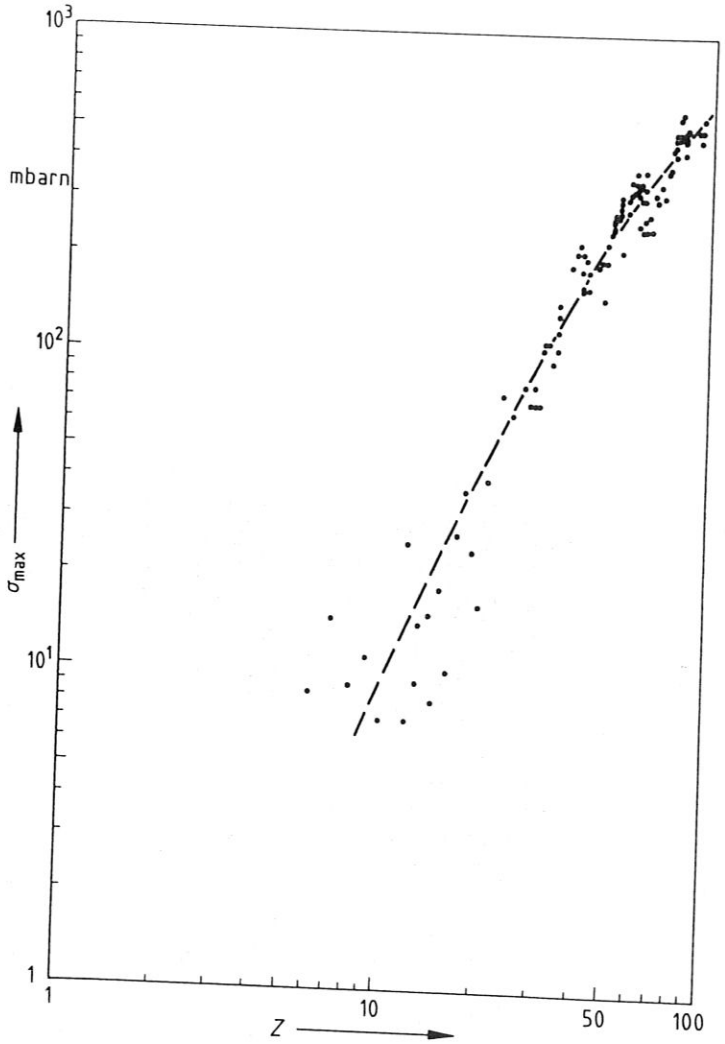

Fig. 2.12: Maximum of the total photoneutron reaction cross section as a function of the atomic number

The average width of the photoneutron cross section curve is about 6 MeV which is many orders of magnitude higher than the level width of a single excited nuclear state. This is the reason for the expression "giant resonance".

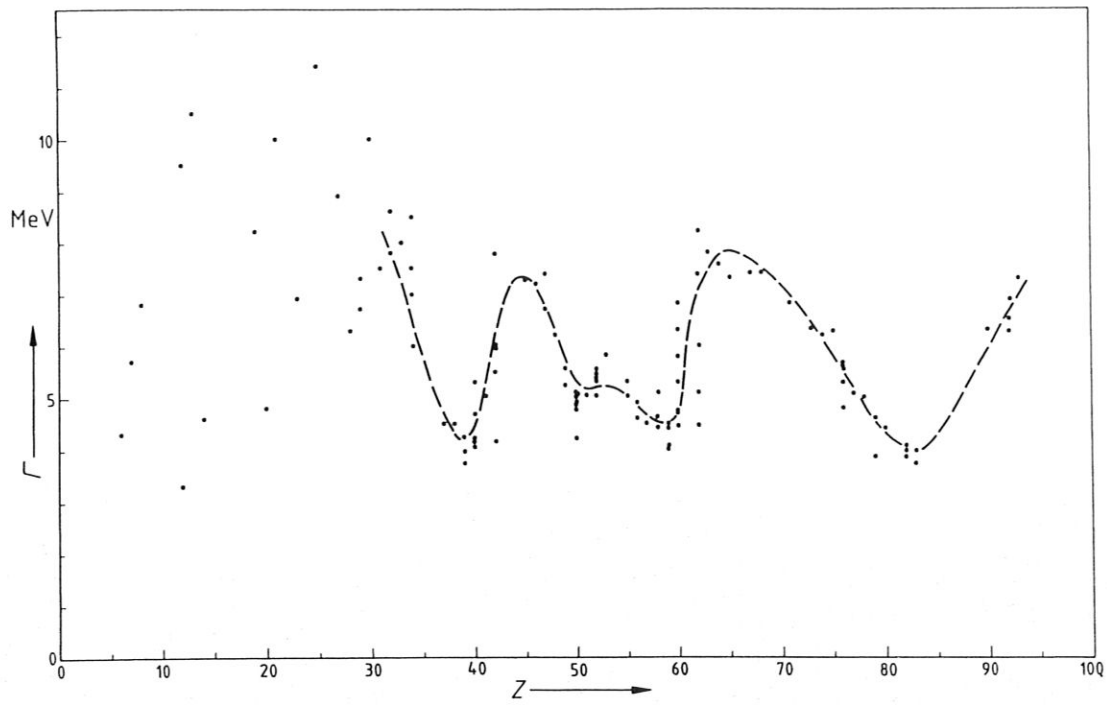

Fig. 2.13: Full width at half maximum (FWHM) of the total photoneutron cross section curve as a function of the atomic number

Since the peak cross section strongly increases with the atomic number of the nuclide the same must be true for the integrated cross section:

$$\sigma_{int}(\gamma, \text{tot n}) = \int_0^\infty \sigma(\gamma, \text{tot n})\,dE \qquad (2.12)$$

For medium and heavy nuclei the total photoneutron cross section nearly equals the photon absorption cross section. Therefore eq. (2.6) should give a reasonable estimation not only for the integrated absorption cross section but also for the integrated total photoneutron cross section. Fig. 2.14 shows indeed that for Z $\gtrsim$30 eq. (2.6) represents a remarkably good description of the integrated total photoneutron cross section. For the light nuclei, however, the experimental data are much below the theoretical curve. This can be explained having in mind that for low atomic number the emission of charged particles - especially protons - significantly contributes to the total reaction cross

section, but this partial cross section is not included in the total photoneutron cross section.

2.3.1 (γ,n)-reactions

The most important contribution to the total photoneutron cross section in the giant resonance region is the single neutron emission from the excited nucleus (compare the corresponding integrated cross sections in Fig. 2.14[128,129]).

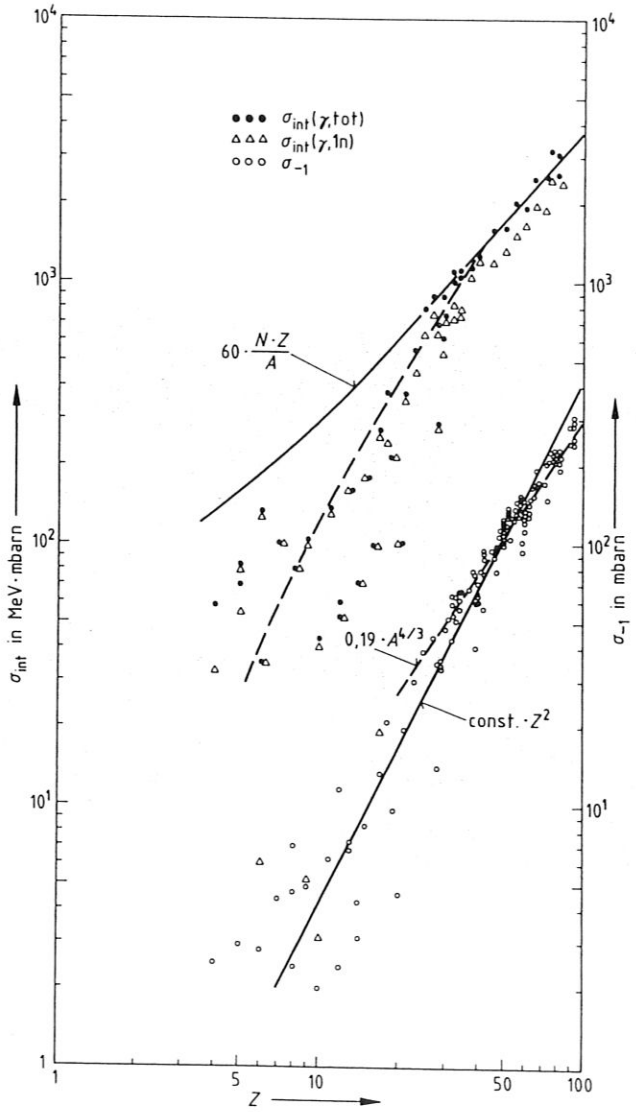

Fig. 2.14: Integrated photoneutron cross section as a function of the atomic number; σ_{-1} - integral of the total photoneutron cross section weighted with the $^1/_e$ - photon spectrum (this roughly describes the bremsstrahlung spectrum)

Consequently, the giant resonance structure is clearly pronounced in the $(\gamma,1n)$ cross sections, too. Of course the resonance parameters are slightly different from those of the total photoneutron cross section. In Fig. 2.6 to Fig. 2.9 measured single photoneutron cross sections

$$\sigma(\gamma,1n) = \sigma(\gamma,n) + \sigma(\gamma,np) \tag{2.13}$$

are plotted. Especially for medium and heavy nuclei this partial cross section is nearly identical with the (γ,n)-cross section because proton emission is severely hindered by the coulomb barrier (see 2.3.3).

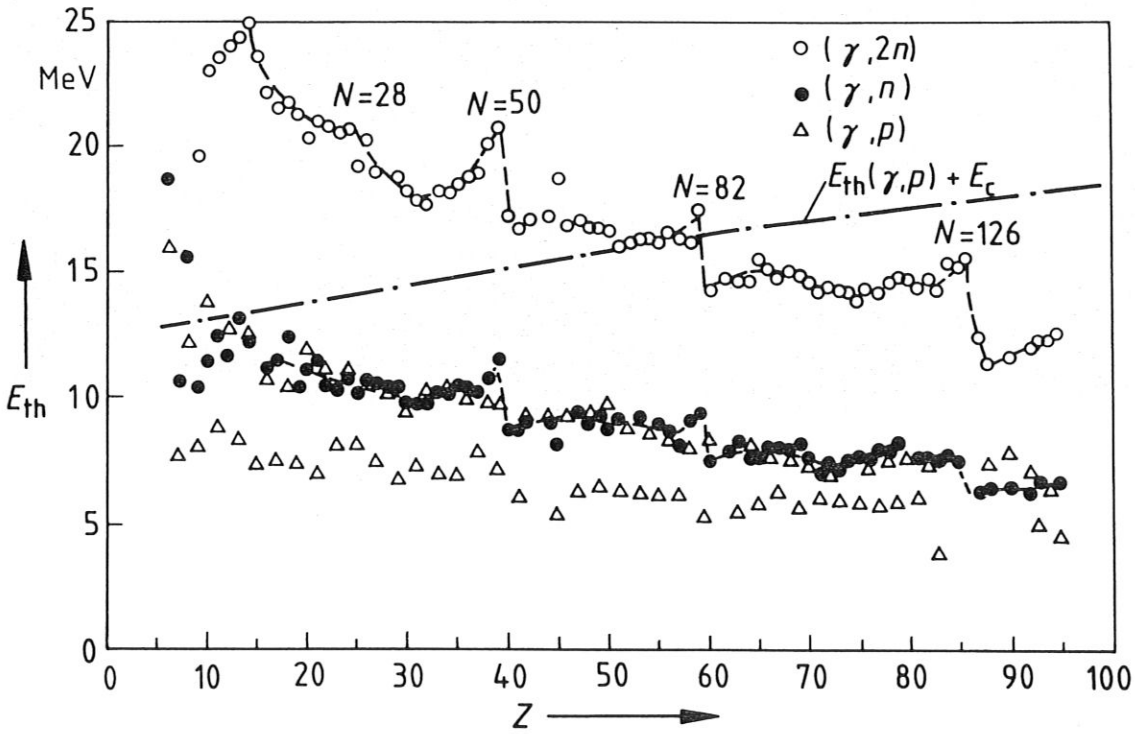

Fig. 2.15: Threshold energies of photonuclear reactions as a function of the atomic number; E_c - Coulomb barrier

In the analytically most important (γ,n)-reaction the only particle emitted from the excited nucleus is one neutron. The threshold of the (γ,n)-reaction is identical with the binding energy of the neutron to the nucleus.

The (γ,n)-threshold plotted in Fig. 2.15 as a function of the atomic number of the target nucleus shows a relatively smooth decrease from more than 15 MeV for light nuclei down to about 8 MeV for heavy nuclei. At several values of the atomic number slight discontinuities exist which reflect the nuclear shell structure. They are more pronounced for the $(\gamma,2n)$-threshold values.

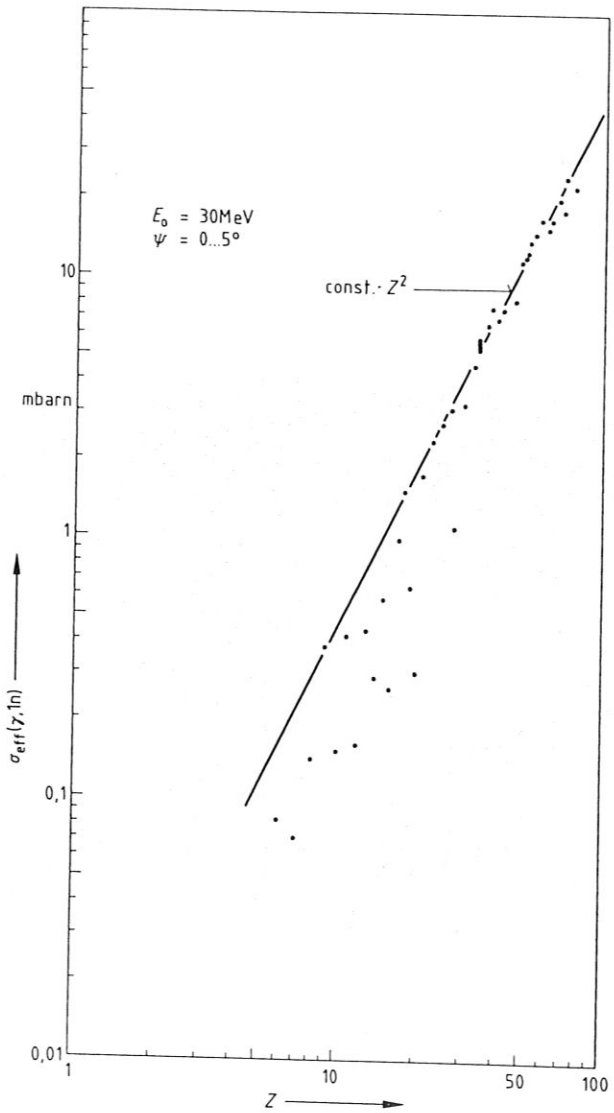

Fig. 2.16: Effective cross sections of (γ,n)-reactions as a function of the atomic number for 30 MeV-bremsstrahlung emitted from a heavy metal target in the angular range of Ψ = 0 - 5 degrees (see Eq. 1.15)

For analytical purposes the achievable specific saturation activity is an interesting value. It is proportional to the effective cross section of the nuclear reaction (see Ch.1, Eq. 1.15):

$$\sigma_{eff} = \int_{E_{th}}^{E_{max}} f(E) \cdot \sigma(E) dE \qquad (2.14)$$

f(E) = normalised spectrum of the activating photons (weighting function; see Fig. 1.1)

In Fig. 2.16 the effective cross section of (γ,n)-reactions is plotted as a function of the atomic number for bremsstrahlung produced by stopping a 30 MeV electron beam in a heavy metal target. As expected the bremsstrahlung weighted cross section also rapidly increases with the atomic number. For medium and heavy nuclei it is approximately proportional to the square of the atomic number. Thus, by irradiating heavy elements in a photon beam much higher activities can be produced than in light elements.

2.3.2 $(\gamma,2n)$- and $(\gamma,3n)$-reactions

Sometimes no analytically suitable radionuclides are produced in a given element by (γ,n)-reactions. Then higher order reactions such as $(\gamma,2n)$ or even $(\gamma,3n)$ must be used. The threshold energies for $(\gamma,2n)$-reactions, however, are nearly twice as high as those of (γ,n)-reactions (Fig. 2.15) and the peak cross sections are considerably lower (Fig. 2.6 to Fig. 2.10). Therefore, the achievable saturation activities and consequently the analytical sensitivity are much lower than for (γ,n)-reactions. If an electron accelerator is used as a photon source the induced acitivity can be increased by using a higher electron energy because the effective cross section increases with the bremsstrahlung energy due to a better overlap of the photon spectrum with the cross section curve.

2.3.3 Reactions with emission of charged particles

The emission of charged particles from an excited nucleus is hindered by nuclear forces and by the Coulomb barrier. The attracting nuclear forces are responsible for the binding energy of the particle which is identical with the threshold energy of the photonuclear reaction. Even if the photon energy exceeds the binding energy of the charged particle its emission probability re-

mains very low because it is enclosed in an electrostatic potential wall called Coulomb barrier. Nevertheless, there is a non-zero probability for the particle to be transmitted through this barrier by the quantum mechanical tunnel effect. As a consequence, the photonuclear cross section for charged reaction products very slowly rises above the threshold and then strongly increases as the photon energy exceeds the coulomb barrier.

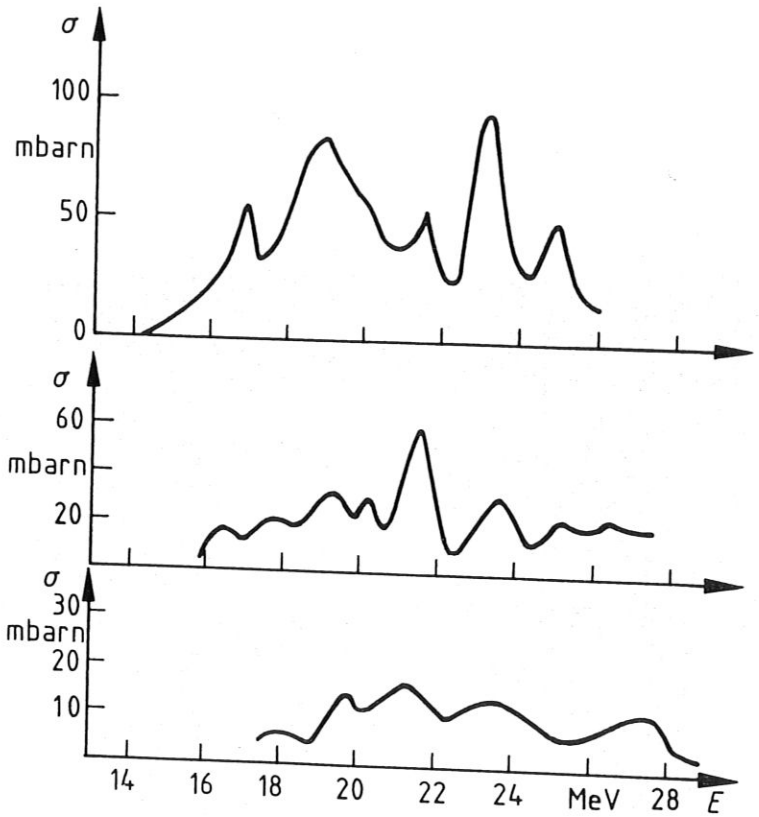

Fig. 2.17: Photoproton cross sections for ^{58}Ni (upper curve), ^{60}Ni and ^{62}Ni (lower curve); after Miyase et al.[1138]

As an example, in Fig. 2.17 measured (γ,p)-cross sections of the most abundant stable nickel isotopes are plotted. In comparing the effective threshold energies (see next page) with the proton binding energies we conclude that the Coulomb barrier height must be about 6 MeV which is in good agreement with theory. From Fig. 2.15 we see that the (γ,p)-thresholds are equal or less than the (γ,n)-values. In addition the average effective threshold energies are plotted

$^{58}Ni(\gamma, p)^{57}Co \quad E_{th} = 8.2$ MeV

$^{60}Ni(\gamma, p)^{59}Co \quad E_{th} = 9.5$ MeV

$^{62}Ni(\gamma, p)^{61}Co \quad E_{th} = 11.1$ MeV

which were calculated by adding the Coulomb barrier to the proton binding energy. Since the height of the coulomb barrier rises with increasing atomic number the effective threshold also increases in contrast to the (γ,n)-threshold. Due to the high effective threshold and the low cross section it is difficult to observe $(\gamma,$charged particle$)$-reactions for heavy nuclei. For analytical purposes these reactions are important only in the case of light and medium elements (except very few heavier elements; see Ch.5). In several advantageous cases $(\gamma,$charged particle$)$-reactions have been utilised for the production of carrier-free radionuclides; see e.g. Ref's.[130-136].

2.4 Yields of photonuclear reactions

The yield of a photonuclear reaction may be defined in many different ways with regard to the irradiation time and the other physical irradiation parameters. From the physical point of view the activity at saturation which would correspond to infinite irradiation time is the most significant value because it is identical with the reaction rate.

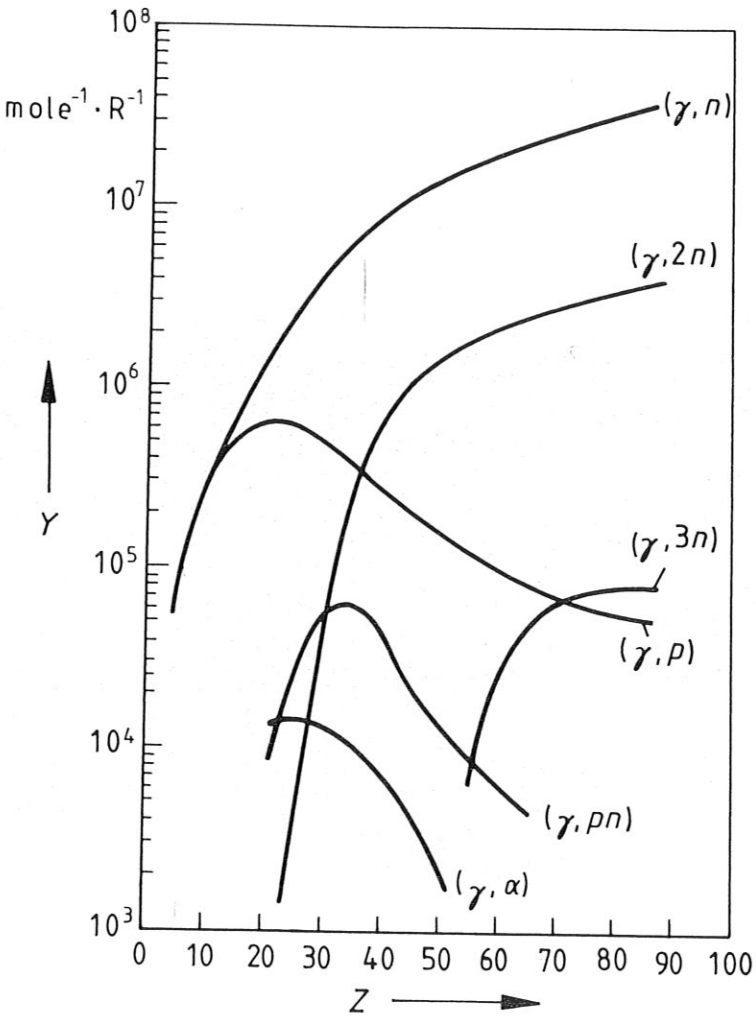

Fig. 2.18: Yields of photonuclear reactions for 30 MeV-bremsstrahlung as a function of the atomic number (explanations see text; after Kato[911])

If the saturation activity is divided by the irradiated mass of the target nuclide and the flux density of the activating photons we immediately obtain - apart from a constant - the effective cross section of the reaction (see Eq. 1.15) which can be interpreted physically. For analytical applications it is more appropriate to use the activity at the end of a fixed standard irradiation time for standard irradiation conditions. The first definition is used in Fig. 2.18 in order to compare different photonuclear reaction types. The radiation source was a platinum bremsstrahlung converter bombarded with 30 MeV electrons. From the measured activity the number of radioactive nuclei produced per photon dose (in R) and per mole of the target nuclide was calculated and plotted as a function of the atomic number. Obviously these yield data are identical with the saturation activity (production rate) per photon flux density and mole because the dose rate is proportional to the flux density[137]. Therefore the plotted curves represent the dependency of the effective reaction cross section for 30 MeV bremsstrahlung on the atomic number of the target nuclide. As was discussed above, the yield curves for the reactions by which only neutrons are produced - (γ,n); $(\gamma,2n)$; $(\gamma,3n)$ - motonically rise with increasing atomic number. The (γ,n)-yield is higher by more than a factor of ten than the $(\gamma,2n)$-yield and higher by about three orders of magnitude than the $(\gamma,3n)$-yield. This rapid decrease of the reaction yield with increasing number of emitted neutrons is due to the high thresholds and low cross sections for multiple photoneutron emission. The yield of (γ,p)-reactions is nearly comparable to the (γ,n)-yield up to Z=20, but for high atomic the (γ,p) yield curve rapidly declines and falls below the $(\gamma,3n)$-curve because of the increasing Coulomb barrier[138-140]. In the case of charged particle emission the yield curve has a pronounced maximum and a monotonic decline towards higher atomic number. The yield values of (γ,np)-, (γ,α)- and $(\gamma,\alpha n)$-reactions are so small that they are useful for analytical applications only in a very limited number of cases[141]; see also 2.3.3 and Ch.5.

In Fig.2.19 and Fig.2.20 measured yield curves for some representative (γ,n)-reactions are shown as a function of the bremsstrahlung energy. Here the disintegration rate per mass of the target element after one hour irradiation is given. The bremsstrahlung converter was a 6 mm thick Pt disc bombarded by a 100 µA electron beam from a linear accelerator. The samples were placed 5 mm behind the photon source in forward direction (direction of the electron beam). Fig. 2.19 shows that in the case of the light elements the specific activity increases by more than a factor of ten from 25 MeV up to 40 MeV bremsstrahlung. This is due to the increase of bremsstrahlung production with increasing electron energy at constant current and to the better overlap of the bremsstrahlung

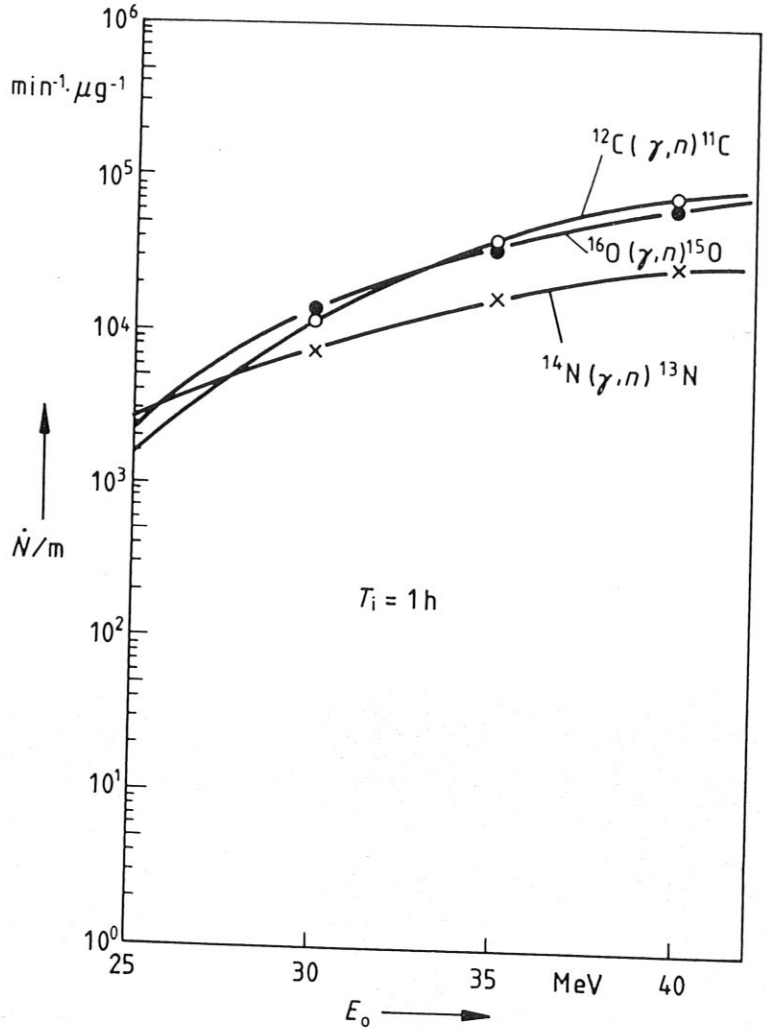

Fig. 2.19: Measured yield curves for (γ,n)-reactions as a function of the maximum bremsstrahlung energy (explanations see text; after Engelmann, Ref's.[23,72])

photon spectrum with the cross section curve (see above). For heavier elements the increase with electron energy is not as steep as for the light elements. Regarding the yield values from Fig.2.19 and Fig.2.20 at 30 MeV we do not observe the monotonic increase with the atomic number as in Fig. 2.18. These differences can be explained if the different decay constants (or half-lives) of the product nuclides are taken into account. If the half-life is much greater than the irradiation time only a small fraction of the maximum activity (saturation value) is achieved whereas for short-lived nuclides the irradiation time

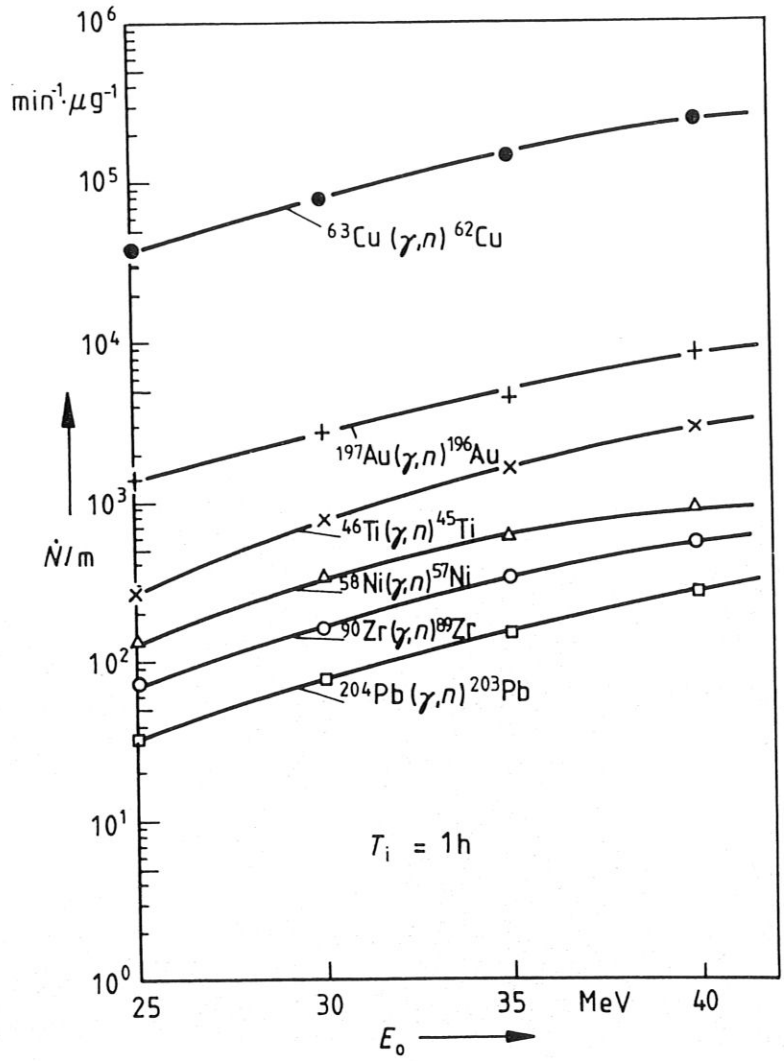

Fig. 2.20: Measured yield curves for (γ,n)-reactions as a function of maximum bremsstrahlung energy (after Engelmann[23,72])

of one hour is sufficiently long for nearly reaching saturation (see Eq.1.17). In the case of the reaction $^{204}Pb(\gamma,n)^{203}Pb$, for example, the effective cross section is very high but on the other hand the half-life of ^{203}Pb (52 h) is much greater than the irradiation time so that only about 1% of the saturation activity is obtained. Another factor is the isotopic composition of the target element. Since the natural abundance of ^{204}Pb is only 1,4% the activity per mass of the target element is further reduced by a large factor. In Fig.2.18, however, the saturation values per mole of the target nuclide are given which do not depend on the irradiation time and the isotopic abundance (see Eq.1.17)

being a direct measure of the effective cross section.

This discussion shows that the achievable analytical sensitivity for the determination of a chemical element does not only depend upon the effective cross section of the photonuclear reaction but also on the ratio between the irradiation time, the half-life of the product nuclide and of the isotopic abundance of the target nuclide in the element to be analysed.

From Fig.2.19 and Fig.2.20 one could conclude that the optimum electron energy for the analysis of an element equals the maximum energy of the available accelator in any case. This is certainly correct regarding the analytical sensitivity in terms of activity yields but there is a severe restriction of the useful electron energy because at very high energies many interfering higher order photonuclear reactions occur which can disturb the analysis, especially the multielement analysis of complex samples[142,143]. Interference reactions can be readily avoided by selecting a sufficently low electron energy where these reactions are still of minor importance. In practice, the optimum irradiation energy is always a compromise between a good analytical sensitivity and sufficiently low interference. For most problems especially in multi-element analysis an electron energy of about 30 MeV has proved to be a reasonable value.

For more detailed information about photonuclear yields the reader might refer to Ref's.[137,144-152].

2.5 Radionuclides produced through photonuclear reactions

2.5.1 Light target elements

From the elements H to B no analytically useful radionuclides are produced. From carbon, nitrogen, oxygen and fluorine pure β^+-emitters are produced by (γ, n)-reactions. These radionuclides cannot be analysed by means of nuclide-specific gamma-rays but only by detecting the unspecific 511 keV annihilation radiation which originates from positrons emitted from radioactive nuclei, absorbed in the surrounding material. In the annihilation process the positron captures an electron from the material thus forming the so-called positronium which then decays by conversion of the positron and electron rest mass (511 keV each) into two 511 keV photons simultaneously emitted into opposite directions. (see Ref.[153]). Since only the 511 keV annihilation radiation is available for the analysis of the light elements up to fluorine in general a chemical separation of these elements must be performed (see Ch.6.1).

2.5.2 Medium and heavy elements

In the case of medium and heavy elements however the radionuclides produced by photonuclear reactions emit - with very few exceptions - gamma-radiation which is characteristic for the nuclide. Due to the specific gamma-radiation an instrumental multi-element analysis of medium and heavy elements using high resolution gamma-ray spectroscopy becomes possible. By photoneutron reactions - (γ,n), (γ,2n), etc. - in general neutron-deficient nuclides are produced from the stable nuclides of the target element. Their predominant decay mode for low atomic number is β^+-emission which leads to excited states of the decay product accompanied with subsequent gamma-ray emission or without gamma emission directly to the ground state (as in the case of ^{11}C, ^{13}N, ^{15}O, ^{18}F). Neutron-deficient radionuclides with medium and high atomic number decay through two competing modes, namely β^+-emission and electron capture (EC). Electron capture in general also leaves the decay product in an excited state which returns to the ground state through gamma-ray emission. Instead of positron emission the nucleus captures an orbital electron - predominantly a K-electron - thus leaving an electron hole in the K-shell. When this hole is subsequently filled by an electron from a higher shell characteristic X-radiation is produced or an Auger-electron is emitted. For heavy nuclei X-ray emission is favoured. The X-ray energy is proportional to the square of the atomic number. In the case of heavy elements X-ray spectroscopy can be used as an alternative to conventional

γ-ray spectroscopy because the X-ray photons have a conveniently high energy (up to about 80 keV) and the emission probability is sufficiently high (see Ch.6.2 and Ref's.[154-161]).

In the case of a target element having several stable isotopes this series of isotopes may be interrupted by one or more β^--emitting radionuclides. Then also β^--emitting radionuclides can be produced from this element through photoneutron reactions and analysed by conventional gamma-ray spectroscopy. The most important production mode of β^--active radionuclides in photon activation analysis, however, is the (γ,p)-reaction which reduces the number of protons in the nucleus so that a neutron-rich radionuclide is generated. In the most cases these radionuclides can be analysed by gamma-ray spectroscopy. There are only a few unfavourable cases in which the reaction product does not emit nuclide specific gamma-rays. In general the nucleus originating from a photonuclear reaction is not produced in its ground state but in an excited state. This excitation energy of the produced nucleus is released by gamma-ray emission. Since the lifetime of the excited states are generally very short this so called prompt gamma-radiation is emitted almost immediately after the formation of the product nucleus thus leaving the nucleus in its ground state. If the ground state of the product nucleus is unstable a radionuclide was produced which is transformed into a decay product. Like the photonuclear reaction the radioactive decay of the product nucleus leads to excited states of the decay product. It is the deexcitation gamma-radiation of the decay product which is normally analysed. In practice, the prompt gamma-radiation from the photoreaction product is not used for analytical purpose because this method would require gamma-ray spectroscopy during irradiation which is exceedingly difficult due to the bremsstrahlung background. However, there are remarkable exceptions. If the reaction product has an isomeric state with sufficiently long half-life the analysis of the gamma-radiation from the reaction product can be performed in the laboratory after irradiation. Particularly simple is the case in which the reaction product is a stable nuclide with an isomeric state. With a certain probability, by the reaction

$$^{136}\mathrm{Ba}(\gamma, \mathrm{n})^{135\mathrm{m}}\mathrm{Ba}$$

the product is formed in the isomeric excited state with 28 h half-life. The 268 kev gamma-radiation from the transition to the ground state of ^{135}Ba can be conveniently measured off-line.

In other cases the reaction product having an isomeric state is unstable. The isomere originating from the photonuclear reaction can transite to its (unstable) ground state, accompanied by gamma emission and then the ground state subsequently is transformed into an excited state of the decay product, followed by gamma-ray emission.

$$^{134}Ba(\gamma, n)^{133m}Ba$$

$$^{133m}Ba \xrightarrow{IT} {}^{133}Ba \quad E_\gamma(IT) = 276\,keV$$

$$^{133}Ba \xrightarrow{EC} {}^{133}Cs \quad E_\gamma = 356\,keV$$

Even longer decay-chains might occur.

Sometimes the isomeric reaction product directly transforms into the decay product: Then only the gamma radiation from the deexcitation of the decay product is observed.

$$^{103}Rh(\gamma, n)^{102m}Rh$$

$$^{102m}Rh \xrightarrow{EC} {}^{102}Ru \quad E_\gamma = 475\,keV$$

Isomeric states exist only in medium and heavy nuclides.

2.5.3 Fissile nuclei

If a fissile nuclide is excited by high energy photons deexcitation through fission of the nuclei may occur. Instead of a single reaction product a broad spectrum of radionuclide ranging from low atomic number up to heavy elements is produced in close analogy to fission induced by thermal neutrons. Most of these products are β^--emitters. Due to the vast variety of radioactive fission products the gamma-ray spectrum from irradiated uranium, e.g., is extremely complex. Therefore, in general the photofission reaction is only of limited value for the analysis of fissile elements. Moreover, the complex gamma-ray spectra of photofission products might appear as a serious interference source if higher concentrations of fissile material are present in the analsed sample (see 6.2).

Another method for measuring the overall concentration of fissile elements in a sample is the detection of neutrons which are also emitted as a consequence of photofission. In contrast to gamma-ray spectroscopy used for the analysis of non-fissile elements this method is not nuclide-specific because the fission-neutrons do not supply any information about their origin. Another drawback is due to the fact that the neutrons must be detected during irradiation (in-beam analysis) which is difficult on account of background problems (see above). Another method for discriminating between different fissile nuclides present in the sample makes use of the different photoneutron thresholds. Here the electron energy of the accelerator and hence the maximum photon energy is varied. When the electron energy passes the threshold of a fissile nuclide the neutrons yield rises. Since the photoneutron yield curves of different fissile nuclides (e.g. ^{232}Th, ^{235}U, ^{238}U, ^{239}Pu) are markedly different near threshold a rough discrimination between different nuclides becomes possible[162]; see also - in a different context - Ref.[181].

Furtherly recommended literature about high energy photon reactions: Ref's[70,163-176].

2.5.4 Neutron-induced reactions

In practical photon activation analysis work one sometimes encounters radionuclides which can only be attributed to neutron-induced reactions. The neutron source responsible for these reactions is the bremsstrahlung converter of the electron accelerator. In the heavy metal of the converter photoneutrons are produced by the bremsstrahlung thus yielding a considerable neutron flux density at the irradiation position of the sample. The shape of the neutron spectrum depends on the material in the vicinity of the bremsstrahlung converter. Besides the primary photoneutrons a large low energy component is produced by moderation of the primary neutrons in the surrounding material. Therefore, two types of neutron-induced reaction may occur in the sample. Low energy neutrons may be captured by (n,γ)-reactions and neutrons with sufficiently high energy may induce threshold reactions e.g. (n,p) or (n,α) processes. By (n,γ)-reactions, in contrast to the complementary (γ,n)-reactions, neutron-rich β^--emitters are produced. This is the neutron reaction type most frequently observed in photon activation analysis. In the case of aluminium (γ,n)- and (γ,p)-reactions do not produce analytically suitable radionuclides. In this case the reactions $^{27}Al(n,p)^{27}Mg$ and $^{27}Al(n,\alpha)^{24}Na$ induced by photoneutrons have been found useful.

Normally reactions with photoneutrons are not analytically exploited because of several difficulties concerning standardisation. This is explained further in 6.2. Moreover, frequently the achievable neutron flux is insufficient for trace analysis. However, in a few cases photoneutrons have been used for activation analysis. E.g., in the authors' laboratory an irradiation position was installed at the accelerator which allows the activation of samples in photoneutron fields with variable cadmium ratios and which are practically free from high energy photon contamination (see Ch.3). The achievable neutron flux density is comparatively poor (several $10^{10} cm^{-2} s^{-1}$); nevertheless, in advantageous cases trace determinations can be performed[177]. For example, routine analyses of several elements in air dust filters have been carried out successfully analysing vanadium and manganese by activation with photoneutrons[178] (see also 6.2).